

Spontaneous population imbalance in two-component Bose and Fermi gases

Shintaro Takayoshi,¹ Masahiro Sato,² and Shunsuke Furukawa^{3,2}

¹*Institute for Solid State Physics, University of Tokyo, Kashiwa, Chiba 277-8581, Japan*

²*Condensed Matter Theory Laboratory, RIKEN, Wako, Saitama 351-0198, Japan*

³*Department of Physics, University of Toronto, Toronto, Ontario M5S 1A7, Canada*

(Dated: July 26, 2021)

We study two-component (or pseudo-spin- $\frac{1}{2}$) Bose or Fermi gases in one dimension, in which particles are convertible between the components. Through bosonization and numerical analyses of a simple lattice model, we demonstrate that, in such gases, a strong intercomponent repulsion induces spontaneous population imbalance between the components, namely, the ferromagnetism of the pseudo spins. The imbalanced phase contains gapless charge excitations characterized as a Tomonaga-Luttinger liquid and gapped spin excitations. We uncover a crucial effect of the intercomponent particle hopping on the transition to the imbalanced phase. In the absence of this hopping, the transition is of first order. At the transition point, the energy spectrum reveals certain degeneracy indicative of an emergent $SU(2)$ symmetry. With an infinitesimal intercomponent hopping, the transition becomes of Ising type. We determine the phase diagram of the model accurately and test the reliability of the weak-coupling bosonization formalism.

PACS numbers: 05.30.Jp, 05.30.Fk, 03.75.Mn, 75.10.Jm

I. INTRODUCTION

Ultracold atomic gases offer highly controllable laboratories for testing and exploring novel many-body phenomena in interacting systems [1, 2]. One line of current interest is to confine atoms to highly elongated traps, effectively creating one-dimensional (1D) systems. In 1D interacting systems, the elementary excitations are collective modes, and the intuition based on the free-particle theory breaks down. For the spinless (one-component) case, theory predicts the equivalence of Bose and Fermi gases; both are described by the Tomonaga-Luttinger liquid (TLL) theory at low energies [3]. As a hallmark example, fermionization of bosons has been observed in a Bose gas of ^{87}Rb atoms tuned into a strongly repulsive regime [4, 5]. Another frontier of activity is the creation of multicomponent gases using different internal states of atoms or using different species of atoms. If we limit our attention to 1D systems, a two-component Bose gas composed of the two hyperfine states of ^{87}Rb has been confined in a 1D trap [6, 7]. Even without internal states, one can load the atoms in a double-channel trap [8–10] [Fig. 1(b)] or on a ladder-type lattice [11, 12], effectively creating a 1D two-component gas. These two-component gases are expected to display a variety of phases depending on the intra- and intercomponent interactions. In a double-channel or ladder structure, in particular, the magnitudes of these two interactions would be different essentially and controllable separately.

In this paper, we study the two-component Bose or Fermi gases in one dimension and analyze a quantum phase transition induced by a strong intercomponent repulsion. In two-component gases consisting of two species of atoms, it has been argued that a strong intercomponent repulsion induces the phase separation (the demixing) of the species (see, e.g., Refs. 13–19). Here we consider an analogous instability in the different situa-

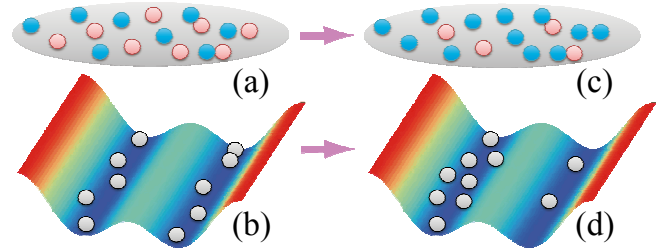


FIG. 1: (Color online) Illustrations of 1D two-component gases. The two components represent two internal states of atoms [shown by different colors in (a) and (c)]. Even without internal states, a double-channel trap potential can produce a similar situation [(b) and (d)]. A strong repulsion between the components induces the population imbalance [(c) and (d)].

tion where the two components represent two (internal) states of single-species atoms and thus particles are mutually *convertible* between the components. The system has a \mathbb{Z}_2 symmetry with respect to the interchange of the two components. In this case, it is expected that, under a strong intercomponent repulsion, a single component can dominate the whole system (population imbalance) as in Figs. 1(c) and 1(d). The \mathbb{Z}_2 symmetry is spontaneously broken while the translational symmetry is retained. This ordering may also be viewed as ferromagnetism if we identify the two components with the pseudo spin $\frac{1}{2}$. A notable point in the present setting is that differently from the case of two-species mixtures, an intercomponent particle hopping can exist and violate the separate conservation of particle number in each component. It is also worth noting that the mechanism of spontaneous imbalance is in fact ubiquitous in nature. It underlies the ferromagnetism in $U(1)$ -symmetric itinerant electrons [20], the vector chiral order in some frus-

trated magnets [21, 22], and the spontaneous rotation of a trapped Bose gas [23]. This mechanism can occur both on a lattice and in a continuum since it does not involve any crystallization.

In spite of their simplicity and ubiquity, the basic properties of the spontaneous imbalance and related phenomena have been rather poorly understood. Mean-field analyses of coupled Gross-Pitaevskii equations [13] cannot capture the effects of strong quantum fluctuations in one dimension. A study beyond the mean-field argument has been done based on the weak-coupling bosonization formalism [14]. In this formalism, each component is described as a TLL, and the intercomponent coupling is perturbatively treated. Then, as will be explained in Sec. III, the spontaneous imbalance is predicted to occur at a point where one of the TLL parameters diverges and this formalism breaks down [14]. Therefore, this formalism cannot be used to describe the imbalanced phase nor the transition to it.

Recently, 1D spin-polarized (ferromagnetic) Bose gases in a strongly repulsive regime have been studied actively using integrable models [24, 25] and effective field theories [26–29]. In these studies, the original Hamiltonian has $SU(2)$ symmetry in terms of the (pseudo) spins, and this symmetry is spontaneously broken. In this setting, the excitations consist of a gapless charge mode characterized as a TLL and a gapless spin wave mode with a quadratic dispersion. In contrast, in our present setting, the (pseudo) spin $SU(2)$ symmetry is reduced to \mathbb{Z}_2 . The low-energy excitation structure in such a reduced-symmetry case has not been addressed. Furthermore, these studies of $SU(2)$ -symmetric systems focus only on the properties of the fully polarized state, and the nature of the ferromagnetic (population-imbalance) transition has not been discussed.

In this paper, we analyze a simple lattice model of a 1D two-component Bose or Fermi gas to address the basic properties of the spontaneous population imbalance. We use two numerical methods, exact diagonalization and infinite time-evolving block decimation [30], in efficient manners to go beyond the existing effective theories. We determine the phase diagram accurately and test the reliability of the bosonization prediction. Using the scaling of the entanglement entropy, we demonstrate that the low energy physics of the imbalanced phase is described by a one-component TLL, indicating that the excitations consist of a gapless charge mode and a gapped spin mode. We uncover a crucial effect of the intercomponent particle hopping on the nature of the transition. Perturbation theory from the strong-coupling limit in the half-filled case provides a qualitative understanding of the phase diagram and the nature of the transition.

II. MODEL

We start from a two-component Bose gas model on a 1D lattice defined by the Hamiltonian

$$\begin{aligned} \mathcal{H} = & \sum_{r=1,2} \sum_{j=1}^L [-t(b_{r,j}^\dagger b_{r,j+1} + \text{H.c.}) + V n_{r,j} n_{r,j+1} \\ & + U_0 n_{r,j} (n_{r,j} - 1) - \mu n_{r,j}] \\ & + \sum_{j=1}^L [-t'(b_{1,j}^\dagger b_{2,j} + \text{H.c.}) + U n_{1,j} n_{2,j}], \end{aligned} \quad (1)$$

where $b_{r,j}$ is a bosonic annihilation operator at site j in the r th component, and $n_{r,j} = b_{r,j}^\dagger b_{r,j}$ is the number operator defined from it. The first and second lines represent hopping and potential terms in each component, and the third represents those between the components. We set $t \geq 0$ and $t' \geq 0$. (The choices of the signs are arbitrary under gauge transformation.) For simplicity, we consider the hard-core limit $U_0 \rightarrow \infty$, where two particles in the *same* component cannot occupy the same site j (but those in *different* components can).

We are also interested in the two-component fermionic model which is defined by replacing all the bosonic operators $b_{r,j}$ in Eq. (1) by fermionic operators $f_{r,j}$. In the fermionic model, the hard-core interaction U_0 automatically drops out. When $t' = 0$, the hard-core bosonic model is equivalent to the fermionic one via the Jordan-Wigner transformation:

$$f_{1,j} = \exp \left[i\pi \sum_{l=1}^{j-1} n_{1,l} \right] b_{1,j}, \quad (2a)$$

$$f_{2,j} = \exp \left[i\pi \left(\sum_{l=1}^L n_{1,l} + \sum_{l=1}^{j-1} n_{2,l} \right) \right] b_{2,j}, \quad (2b)$$

where the “string” part runs first in the first component and then in the second component. Because of this correspondence, the bosonic and fermionic models can be analyzed in parallel for $t' = 0$. At the special point $t' = V = 0$, the model (1) is equivalent to the solvable fermionic Hubbard chain, where the labels $r = 1$ and 2 are identified with spin-up and spin-down states, respectively. In this case, the population imbalance is known not to occur.

When $t' \neq 0$, the bosonic and fermionic models are no longer equivalent. For the following reasons, however, they are expected to display essentially the same physics. Specifically, we consider a different Jordan-Wigner transformation:

$$f_{1,j} = \exp \left[i\pi \sum_{l=1}^{j-1} (n_{1,l} + n_{2,l}) \right] b_{1,j}, \quad (3a)$$

$$f_{2,j} = \exp \left[i\pi \left(\sum_{l=1}^j n_{1,l} + \sum_{l=1}^{j-1} n_{2,l} \right) \right] b_{2,j}, \quad (3b)$$

where the “string” part now runs alternately between the two components. Under this transformation, the intra-component hopping terms are transformed as

$$b_{1,j}^\dagger b_{1,j+1} = e^{i\pi n_{2,j}} f_{1,j}^\dagger f_{1,j+1}, \quad (4a)$$

$$b_{2,j}^\dagger b_{2,j+1} = e^{i\pi n_{1,j+1}} f_{2,j}^\dagger f_{2,j+1}, \quad (4b)$$

while other terms in Eq. (1) retain the same form. In the low- (respectively high-) density limit, the phase factors $e^{i\pi n_{r,i}}$ in Eq. (4) are fixed essentially at unity (respectively -1). At half-filling and for strong intercomponent repulsion, the intracomponent hopping t does not contribute in the first-order perturbation theory, as explained in Sec. V. Therefore, at least in these cases, the bosonic and fermionic models lead to the same physics.

III. WEAK-COUPLING THEORY

We formulate a weak-coupling bosonization theory for the hard-core boson model (1), and discuss the instability of the two-component TLLs following Ref. 14. When $t' = U = 0$, the model decouples into two independent Bose gases, each equivalent to a solvable spin- $\frac{1}{2}$ XXZ chain in a magnetic field. For $-2 < V$ and $0 < \langle n_{r,j} \rangle < 1$, each component $r (= 1, 2)$ obeys a TLL described by the Hamiltonian [3]

$$\mathcal{H}_r^{\text{eff}} = \int dx \frac{v}{2} [K(\partial_x \theta_r)^2 + K^{-1}(\partial_x \phi_r)^2], \quad (5)$$

where θ_r and ϕ_r are a dual pair of scalar fields, and $x = ja_0$ with a_0 being the lattice spacing. The group velocity v and the TLL parameter K can be determined from Bethe ansatz [3]. To treat t' and U terms as perturbations, we use the following bosonization formulas:

$$n_{r,j} = \rho_0 - a_0 \partial_x \phi_r(x) / \sqrt{\pi} + \dots, \quad (6a)$$

$$b_{r,j}^\dagger = \exp[-i\sqrt{\pi} \theta_r(x)] (B_0 + \dots), \quad (6b)$$

where $\rho_0 = \langle n_{r,j} \rangle$ is the averaged density and B_0 is a nonuniversal constant. Introducing new bosonic fields $\phi_\pm = (\phi_1 \pm \phi_2) / \sqrt{2}$ and $\theta_\pm = (\theta_1 \pm \theta_2) / \sqrt{2}$, we obtain the effective Hamiltonian for Eq. (1),

$$\begin{aligned} \mathcal{H}^{\text{eff}} = & \int dx \sum_{\alpha=\pm} \frac{v_\alpha}{2} [K_\alpha (\partial_x \theta_\alpha)^2 + K_\alpha^{-1} (\partial_x \phi_\alpha)^2] \\ & - \frac{2}{a_0} B_0^2 t' \cos(\sqrt{2\pi} \theta_-) - \sqrt{\frac{2}{\pi}} \rho_0 U \partial_x \phi_+ + \dots, \end{aligned} \quad (7)$$

with

$$v_\pm = v \left(1 \pm \frac{KUa_0}{\pi v} \right)^{\frac{1}{2}}, \quad K_\pm = K \left(1 \pm \frac{KUa_0}{\pi v} \right)^{-\frac{1}{2}}. \quad (8)$$

Here we notice the effective separation of the two sectors, (ϕ_+, θ_+) and (ϕ_-, θ_-) , which are respectively called the

“charge” and “spin” sectors by analogy with the Hubbard chain. In the weak-coupling regime ($0 \leq U \ll v/a_0$), both the sectors remain gapless for $t' = 0$. Finite $t' \neq 0$ opens a gap in the spin sector since the vertex term $\cos(\sqrt{2\pi} \theta_-)$ with scaling dimension $1/(2K_-)$ is always relevant. As U increases, these estimates (8) indicate $v_- \rightarrow 0$ and $K_- \rightarrow \infty$ at

$$U_c = \pi v / (Ka_0). \quad (9)$$

In other words, the coefficient $v_- K_-^{-1}$ of $(\partial_x \phi_-)^2$ in Eq. (7) changes sign at this point. This indicates the breakdown of the bosonization description in the spin sector. If we naively assume the existence of a term $(\partial_x \phi_-)^4$ with a positive coefficient in the effective Hamiltonian, a population-imbalanced state with $\Delta n = \langle n_{1,j} \rangle - \langle n_{2,j} \rangle \approx -a_0 \sqrt{2/\pi} \langle \partial_x \phi_- \rangle \neq 0$ is expected to appear along with the breakdown [20, 23]. Equation (9) gives a naive estimation of the transition point [14, 31]. In the case where a two-component gas consists of two-species atoms, this breakdown corresponds to the demixing instability [14].

IV. NUMERICAL ANALYSES

To go beyond the weak-coupling theory and to address the strong-coupling regime, we employed two numerical methods for the bosonic model (1): exact diagonalization (ED) and infinite time-evolving block decimation (iTEBD) [30]. The iTEBD method generates the ground state of an infinite system through the use of a matrix product state. The precision improves as we increase the matrix dimension χ . To perform a calculation at a fixed filling, the chemical potential μ was iteratively tuned through a feedback control in each iTEBD step. To achieve better convergence of the order parameter, we first performed the iTEBD for large U , where the order parameter is large. Then we gradually decreased U repeatedly using the obtained state as the initial state for the next U . We set $t = 1$ as the energy unit hereafter.

A. $t' = 0$ case

Let us first analyze the case with zero intercomponent hopping $t' = 0$, in which the bosonic model (1) is equivalent to the fermionic one with the same Hamiltonian. In this case, the particle number of each component, $N_r = \sum_j n_{r,j}$, is a good quantum number. Therefore, for a given total particle number $N = N_1 + N_2$, ED can be performed separately for each $\Delta N \equiv N_1 - N_2 = 0, \pm 1, \dots, \pm N$. The lowest eigenenergy in each sector is plotted in Fig. 2(a). We observe a direct change of the ground state from a uniform state $\Delta N = 0$ to a fully imbalanced state $\Delta N = \pm N$ as we increase U . Such an abrupt change of ΔN indicates a first-order transition. All the energy levels cross at the same point $U_c = 9.34$, which suggests an emergent $SU(2)$ symmetry at the transition point. Such an emergent $SU(2)$ symmetry has

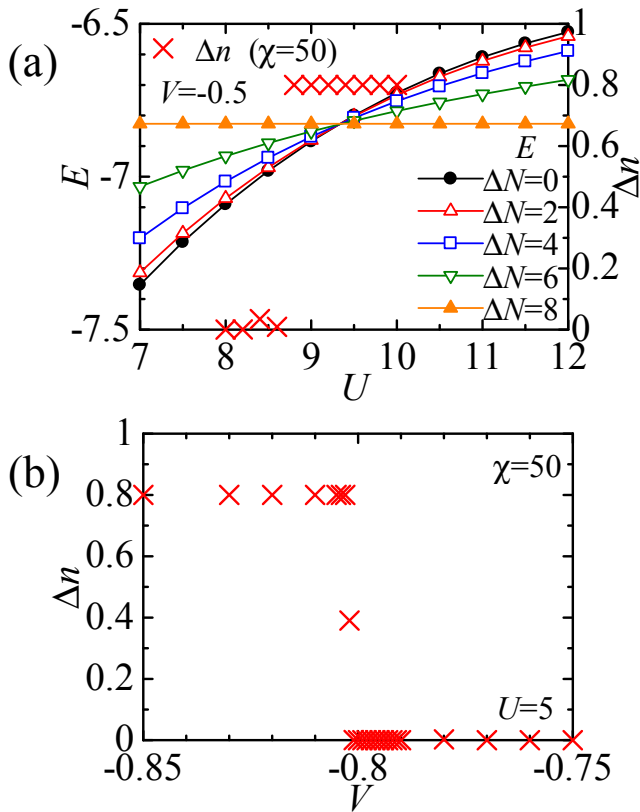


FIG. 2: (Color online) Numerical results for $t' = 0$, $t = 1$, and filling=0.4. (a) The lowest energy levels for different ΔN obtained from ED and the density difference Δn from iTEBD (with $\chi = 50$), as functions of U . In ED calculations, the finite cluster of chain length $L = 10$ was used. (b) Δn obtained from iTEBD as a function of V .

also been predicted in renormalization group analysis [19]. The recent strong-coupling theories for the $SU(2)$ -symmetric case in Refs. 26–29 are expected to apply at this point. In Figs. 2(a) and 2(b), the density difference Δn evaluated by iTEBD shows a jump at a certain point, which also indicates a first-order transition. The transition points obtained from ED and iTEBD are slightly different, which could be mainly attributed to an inherent hysteresis in iTEBD around a first-order transition point. The level-crossing point in ED shows only a very small dependence on the system size except when the total density is close to zero or unity. Therefore, ED gives the better estimate of the transition point.

B. $t' \neq 0$ case

Now we analyze the effect of intercomponent hopping $t' \neq 0$, in which $N_{1,2}$ are no longer conserved separately. As shown in Fig. 3(a), the order parameter Δn calculated with iTEBD grows continuously as a function of U , indicating a second-order transition. The peak of half-

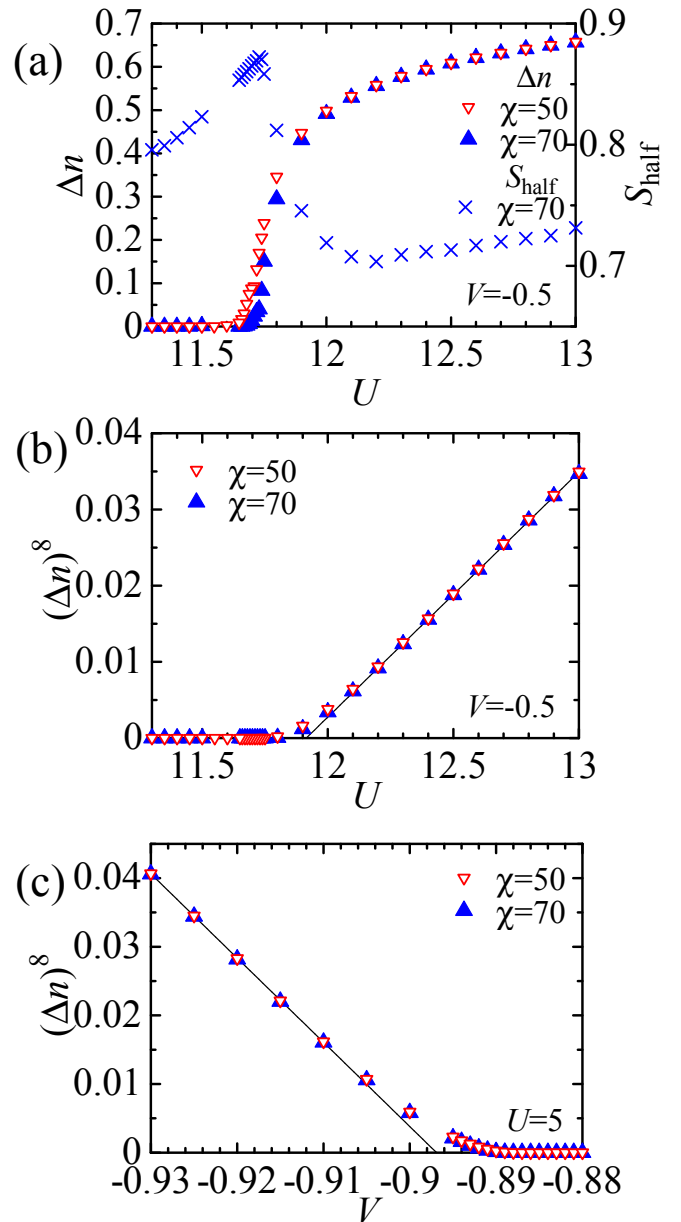


FIG. 3: (Color online) Numerical results for $t' = 0.05$, $t = 1$, and filling=0.4. (a) Density difference Δn and half-chain entanglement entropy S_{half} obtained from iTEBD, as a function of U . The onset of Δn and the peak of S_{half} occur almost simultaneously. (b) $(\Delta n)^8$ versus U , and (c) $(\Delta n)^8$ versus V near the transition point. The black solid lines in (b) and (c) are the linear fits of the data in the imbalanced phase.

chain entanglement entropy S_{half} [see Eq. (5) of Ref. 34 for its definition] gives a reasonable estimate of the transition point. This quantity is known to diverge at a critical point [32, 33], although finite χ introduces a cutoff to the divergence [34]. In Figs. 3(b) and 3(c), $(\Delta n)^8$ is plotted as a function of U and V . The data are well fitted by a linear function except in the very close vicinity of the transition point where χ dependence occurs. This result

indicates the relation $\Delta n \propto (U - U_c)^{1/8} [(V_c - V)^{1/8}]$ along the U [V] axis, in agreement with the critical exponent $\beta = 1/8$ in the 2D Ising universality class [35].

C. Phase diagram

The ground-state phase diagram is summarized in Fig. 4. The left and right sides of the phase boundary correspond to the uniform TLL and imbalanced phases, respectively. The transition points U_c were determined by using the level-crossing point for $t' = 0$ and the peak of S_{half} for $t' \neq 0$. In Fig. 4(a), the phase diagram is symmetric under $n \rightarrow 1 - n$ because of the particle-hole symmetry in the hard-core model. It is found that U_c is shifted to larger values with increasing t' . Namely, the intercomponent hopping diminishes the imbalanced state. Figure 4(b) shows the phase diagram in U - V space. We observe $U_c \rightarrow 0$ as $V \rightarrow -2$. This is naturally expected since, in the decoupled case ($t' = U = 0$), the point $V/t = -2$ corresponds to the two ferromagnetic Heisenberg chains in the spin-system language with $S_{r,j}^z = n_{r,j} - 1/2$. The bosonization prediction (9) and numerical data agree well in this limit. On the other hand, as V is taken to zero, U_c deviates from the bosonization prediction and tends to diverge. For $V \geq 0$, we did not observe a population imbalance, although the bosonization prediction (9) still indicates its occurrence. (We again note that the occurrence of the population imbalance can be disproved in the integrable case $V = t' = 0$.) This indicates intricate roles of U and V on the change of the TLL parameter K_- , which are not covered in the weak-coupling approach.

V. PERTURBATION THEORY IN THE STRONG-COUPLING REGIME

To gain a deeper understanding of the strong-coupling regime, we formulate a perturbation theory in the half-filled case $\langle n_{1,j} \rangle + \langle n_{2,j} \rangle = 1$. In this special case, the charge sector is gapped out and we can thus single out a simple structure in the spin sector. (This procedure is analogous to the derivation of the Heisenberg model from the Hubbard model for a strong on-site repulsion.) In the limit $t/U, t'/U, V/U \rightarrow 0$, the system decouples into independent sites. Each site j has doubly degenerate ground states, $|\uparrow\rangle_j \equiv |n_{1,j} = 1, n_{2,j} = 0\rangle$ and $|\downarrow\rangle_j \equiv |n_{1,j} = 0, n_{2,j} = 1\rangle$. We use these as the basis of the Hilbert space, and we treat t, t' , and V terms as perturbations. First-order perturbation theory is equal to acting the projection operator $P \equiv \prod_j (|\uparrow\rangle_j \langle\uparrow| + |\downarrow\rangle_j \langle\downarrow|)$ on both sides of t, t' , and V terms in Eq. (1). For both the bosonic and fermionic models, the same effective Hamiltonian is obtained as

$$\mathcal{H}_{\text{eff}}^{(1)} = \sum_j (2VT_j^z T_{j+1}^z - 2t'T_j^x), \quad (10)$$

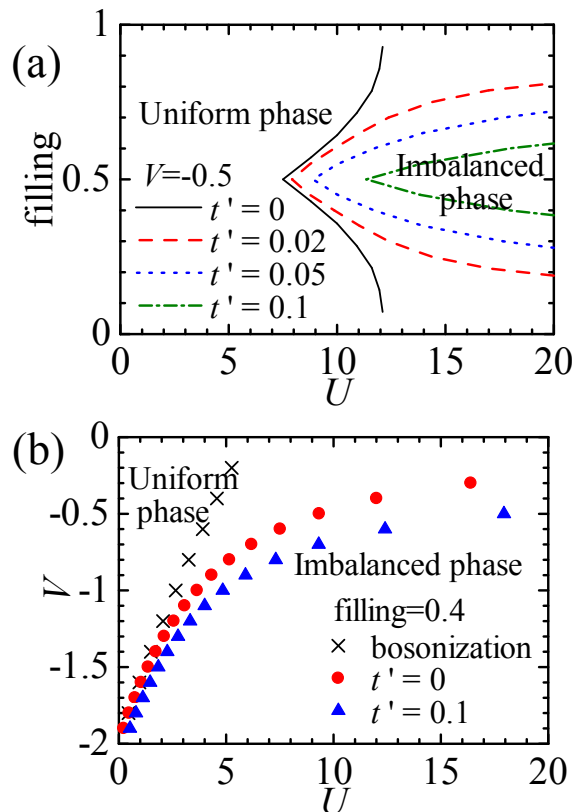


FIG. 4: (Color online) (a) Phase diagram in the U -filling space for $V = -0.5$. We denote the phase boundaries by solid, dashed, dotted, and dash-dotted curves for $t' = 0, 0.02, 0.05$, and 0.1 , respectively. (b) Phase diagram in U - V space for filling = 0.4. The Bosonization prediction (9) of the phase boundary is also shown for comparison.

where T_j^z and T_j^x are pseudo-spin- $\frac{1}{2}$ operators defined as

$$\begin{aligned} T_j^z &\equiv \frac{1}{2} (|\uparrow\rangle_j \langle\uparrow| - |\downarrow\rangle_j \langle\downarrow|) \\ T_j^x &\equiv \frac{1}{2} (|\downarrow\rangle_j \langle\uparrow| + |\uparrow\rangle_j \langle\downarrow|). \end{aligned} \quad (11)$$

For $t' = 0$, Eq. (10) is a classical Ising model. A first-order transition at $V = 0$ separates ferromagnetic ($V < 0$) and antiferromagnetic ($V > 0$) phases. The former is nothing but the population-imbalanced phase. For $t' > 0$, Eq. (10) is equal to an Ising model in a transverse field, which is still solvable. Second-order transitions of Ising type separate ferromagnetic ($V < -2t'$), disordered ($-2t' < V < 2t'$), and antiferromagnetic ($2t' < V$) phases. The presence of t' abruptly changes the nature of the transition, consistent with the numerical results in Figs. 2 and 3. Furthermore, the ferromagnetic phase diminishes as we increase t' , in accordance with Fig. 4. The appearance of the antiferromagnetic phase is due to a lattice effect specific to the half-filled case, and here we do not discuss it further.

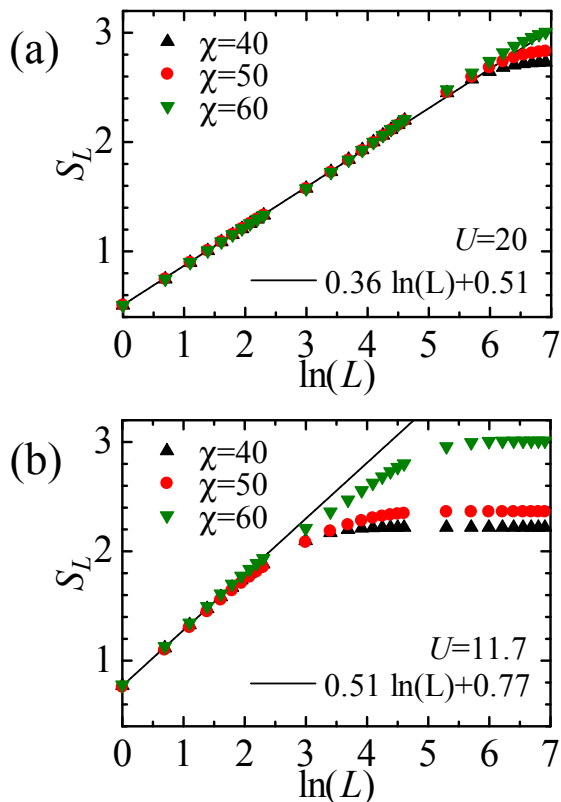


FIG. 5: (Color online) Finite-interval entanglement entropy S_L calculated by iTEBD. We set $t' = 0.05$, $V = -0.5$, and filling=0.4. (a) In the imbalanced phase, we obtain $c \approx 1$. (b) Approximately at the transition point, we obtain $c \approx 1 + 1/2$.

VI. LOW-ENERGY PROPERTIES OF THE IMBALANCED PHASE

We analyze the low-energy properties of the imbalanced phase. In the case of $t' = 0$, it is clear that the low-energy physics is governed by a TLL in the charge sector since the fully polarized state is realized (see Fig. 2). On the other hand, the case of $t' \neq 0$ deserves to be investigated. In the latter case, it is natural to consider the following two possibilities: (i) The effective separation of the charge and spin sectors still holds; the former is described by a TLL while the latter is gapped. (ii) The first chain ($r = 1$) with a dense particle density and the second one ($r = 2$) with a thin density separately form TLLs. To see which possibility is correct, we examine the scaling of the entanglement entropy S_L of the ground state $|\Psi\rangle$. For a finite interval Ω of length L , it is defined as $S_L = -\text{Tr} \rho_\Omega \ln \rho_\Omega$, where $\rho_\Omega = \text{Tr}_{\bar{\Omega}} |\Psi\rangle\langle\Psi|$ is the reduced density matrix on Ω obtained by tracing out the exterior $\bar{\Omega}$. In 1D critical systems, this quantity enables one to determine the central charge c (an indicator of the number of gapless modes) through the formula of a universal

scaling [32, 33],

$$S_L \approx \frac{c}{3} \ln L + \text{const.} \quad (12)$$

Figure 5 shows S_L calculated by combining iTEBD with the transfer matrix technique. Here, an initial state with a fixed number of particles was adopted to achieve better convergence of the wave function. In the imbalanced phase [Fig. 5(a)], $c \approx 1$ is obtained by fitting the numerical data with the scaling formula (12). This supports possibility (i). Namely, the dense and thin components cooperatively form a single TLL. This is strikingly different from a population-imbalanced state extrinsically derived by simply applying a magnetic field (chemical potential difference) for pseudo spins [36]. Figure 5(b) shows the result approximately at the second-order transition point U_c for $t' \neq 0$. Although the data show some χ dependence for large L , the fitting using almost χ -independent data for small L yields $c \approx 1 + 1/2$. This result indicates that an Ising-type transition with $c = 1/2$ occurs in the spin sector while the gapless mode with $c = 1$ in the charge sector remains intact.

VII. CONCLUSIONS

We have studied a simple lattice model (1) of a two-component quantum gas in the strong-coupling regime, using numerical and analytical methods. We demonstrated that the spontaneous population imbalance (ferromagnetism) occurs as we increase the intercomponent repulsion U . We completed the accurate phase diagrams in Fig. 4. It was found that the spontaneous imbalance occurs only for $V < 0$ and that the intercomponent hopping t' diminishes the imbalanced phase. While these intricate roles of V and t' cannot be covered in weak-coupling bosonization theory, perturbation theory from the strong-coupling limit for the half-filled case provides simple qualitative explanations of them.

We have also uncovered the basic properties of the imbalanced phase and the transition to it. Using the scaling of the entanglement entropy, we demonstrated that the low-energy property in the imbalanced phase is governed by a one-component TLL, indicating the separation of gapless charge and gapped spin modes. This is in sharp contrast to the integrable fermionic Hubbard chain, where both the charge and spin sectors behave as TLLs even in the strong-coupling regime [37]. The transition to the imbalanced phase is of first order when $t' = 0$ and of Ising type when $t' \neq 0$. In spite of this drastic effect in the spin sector, the t' term does not spoil the gapless property of the charge sector. At the first-order transition point for $t' = 0$, the energy spectrum reveals a certain degeneracy indicative of an emergent $SU(2)$ symmetry.

Although our analyses are done mainly for the bosonic model, we expect that the fermionic model also displays essentially the same physics as we discussed in Sec II.

For $t' = 0$, the bosonic and fermionic models are exactly equivalent. For $t' \neq 0$, the t' term in the fermionic case has a different bosonization expression and thus a different scaling dimension from the bosonic case in Eq. (7). We expect that, when this term is irrelevant (respectively relevant), the transition between the uniform TLL and imbalanced phases is of first order (respectively of Ising type). In particular, even in the presence of the t' term, the bosonic and fermionic cases become asymptotically equivalent (i) in the low- and high-density limits and (ii) in the strong-coupling limit in the half-filled case.

Releasing the hard-core constraint and discussing the occurrence of the population imbalance in more realistic situations are interesting future directions. We expect that the basic features of the imbalanced phase and the transition uncovered in the present work are robust, irrespective of the microscopic details.

S.T. and M.S. were supported by Grants-in-Aid by JSPS (Grant No. 09J08714) and for Scientific Research from MEXT (Grant No. 21740295 and No. 22014016), respectively.

-
- [1] I. Bloch, J. Dalibard, and W. Zwerger, *Rev. Mod. Phys.* **80**, 885 (2008).
- [2] S. Giorgini, L. P. Pitaevskii, and S. Stringari, *Rev. Mod. Phys.* **80**, 1215 (2008).
- [3] T. Giamarchi, *Quantum Physics in One Dimension* (Oxford University Press, New York, 2004).
- [4] T. Kinoshita, T. Wenger, and D. S. Weiss, *Science* **305**, 1125 (2004).
- [5] B. Paredes, A. Widera, V. Murg, O. Mandel, S. Fölling, I. Cirac, G. V. Shlyapnikov, T. W. Hänsch, and I. Bloch, *Nature (London)* **429**, 277 (2004).
- [6] J. M. McGuirk, H. J. Lewandowski, D. M. Harber, T. Nikuni, J. E. Williams, and E. A. Cornell, *Phys. Rev. Lett.* **89**, 090402 (2002).
- [7] A. Widera, S. Trotzky, P. Cheinet, S. Fölling, F. Gerbier, I. Bloch, V. Gritsev, M. D. Lukin, and E. Demler, *Phys. Rev. Lett.* **100**, 140401 (2008).
- [8] S. Hofferberth, I. Lesanovsky, B. Fischer, J. Verdu, and J. Schmiedmayer, *Nature Phys.* **2**, 710 (2006).
- [9] S. Hofferberth, I. Lesanovsky, B. Fischer, T. Schumm, and J. Schmiedmayer, *Nature (London)* **449**, 324 (2007).
- [10] G.-B. Jo, J.-H. Choi, C. A. Christensen, Y.-R. Lee, T. A. Pasquini, W. Ketterle, and D. E. Pritchard, *Phys. Rev. Lett.* **99**, 240406 (2007).
- [11] J. J. García-Ripoll, M. A. Martin-Delgado, and J. I. Cirac, *Phys. Rev. Lett.* **93**, 250405 (2004).
- [12] J. Sebby-Strabley, M. Anderlini, P. S. Jessen, and J. V. Porto, *Phys. Rev. A* **73**, 033605 (2006).
- [13] T.-L. Ho and V. B. Shenoy, *Phys. Rev. Lett.* **77**, 3276 (1996).
- [14] M. A. Cazalilla and A. F. Ho, *Phys. Rev. Lett.* **91**, 150403 (2003).
- [15] L. Pollet, M. Troyer, K. VanHoucke, and S. M. A. Rollets, *Phys. Rev. Lett.* **96**, 190402 (2006).
- [16] L. Mathey, *Phys. Rev. B* **75**, 144510 (2007).
- [17] T. Mishra, R. V. Pai, and B. P. Das, *Phys. Rev. A* **76**, 013604 (2007).
- [18] A. Hu, L. Mathey, I. Danshita, E. Tiesinga, C. J. Williams, and C. W. Clark, *Phys. Rev. A* **80**, 023619 (2009).
- [19] A. K. Kolezhuk, *Phys. Rev. A* **81**, 013601 (2010).
- [20] K. Yang, *Phys. Rev. Lett.* **93**, 066401 (2004).
- [21] A. Kolezhuk and T. Vekua, *Phys. Rev. B* **72**, 094424 (2005).
- [22] M. Sato and T. Sakai, *Phys. Rev. B* **75**, 014411 (2007).
- [23] A. Tokuno and M. Sato, *Phys. Rev. A* **78**, 013623 (2008).
- [24] E. Eisenberg and E. H. Lieb, *Phys. Rev. Lett.* **89**, 220403 (2002).
- [25] J. N. Fuchs, D. M. Gangardt, T. Keilmann, and G. V. Shlyapnikov, *Phys. Rev. Lett.* **95**, 150402 (2005).
- [26] S. Akhanjee and Y. Tserkovnyak, *Phys. Rev. B* **76**, 140408(R) (2007).
- [27] M. B. Zvonarev, V. V. Cheianov, and T. Giamarchi, *Phys. Rev. Lett.* **99**, 240404 (2007); *Phys. Rev. Lett.* **103**, 110401 (2009).
- [28] K. A. Matveev and A. Furusaki, *Phys. Rev. Lett.* **101**, 170403 (2008).
- [29] A. Kamenev and L. I. Glazman, *Phys. Rev. A* **80**, 011603(R) (2009).
- [30] G. Vidal, *Phys. Rev. Lett.* **98**, 070201 (2007).
- [31] Recently, an improved estimation of the transition point beyond simple bosonization was argued in Ref. 19.
- [32] G. Vidal, J. I. Latorre, E. Rico, and A. Kitaev, *Phys. Rev. Lett.* **90**, 227902 (2003).
- [33] P. Calabrese and J. Cardy, *J. Stat. Mech.* (2004) P06002.
- [34] F. Pollmann, S. Mukerjee, A. M. Turner, and J. E. Moore, *Phys. Rev. Lett.* **102**, 255701 (2009).
- [35] In Ref. 21, an Ising-type transition was predicted to occur between the vector chiral phase and the nematic liquid phase (called the even-odd phase in Ref. 21) in the zigzag spin- $\frac{1}{2}$ chain in a magnetic field. We comment that this Ising transition is essentially different from the one we found in the present case. In the bosonization formalism, different bosonic fields are locked in the nematic liquid and uniform TLL phases.
- [36] Population imbalanced Fermi gases obtained by applying a magnetic field are currently an active topic and are reviewed in, e.g., Sec. IX of Ref. 2.
- [37] M. Ogata and H. Shiba, *Phys. Rev. B* **41**, 2326 (1990).